Ablation of Intraocular Tissue with Fiber-optic Probe–Delivered 266-nm and 213-nm Laser Energy

Xiao-Bo Yu,[1,2] *Joseph Miller,*[1] *Paula K. Yu,*[1] *Stephen J. Cringle,*[1] *Chandrakumar Balaratnasingam,*[1] *William H. Morgan,*[1] *and Dao-Yi Yu*[1]

Purpose. To explore the tissue ablation properties of pulsed 266-nm and 213-nm laser radiation in porcine retina and the potential for 213-nm laser radiation to cut through human trabecular meshwork.

Methods. Segments of porcine retinas were used, and localized areas of tissue were exposed to 266-nm or 213-nm laser. Human trabecular meshwork from donor eyes was also ablated using pulsed 213-nm laser. Ocular tissue was bathed in fluid to mimic the intraocular environment. Single or multiple pulses at various fluence levels were delivered with a tapered fiber-optic probe. The tissue was then fixed for histologic examination. Ablation depth and extent of damage were measured and related to fluence level and number of pulses applied.

Results. Ablation of the inner retina was achieved by single pulses at fluence levels of 0.6 J/cm^2 and higher with 266-nm laser radiation and 0.2 J/cm^2 and higher with 213-nm laser radiation. At the same fluence, ablation depth was greater ($P < 0.001$) with 213-nm than 266-nm laser, with less collateral damage. Ablation of human trabecular meshwork using 213-nm laser was highly dependent on fluence after exposure to single and multiple pulses, allowing good control of ablation depth.

Conclusions. Laser radiation at 213 nm has greater ablation efficiency, less collateral damage, and a more linear dose-response than ablation at 266 nm. Precise removal of human trabecular meshwork was demonstrated using pulsed 213-nm laser radiation. (*Invest Ophthalmol Vis Sci.* 2009;50:3729–3736) DOI:10.1167/iovs.08-3109

Ultraviolet (UV) laser ablation is used in the treatment of corneal refractive disorders but may be of use in the surgical management of vitreoretinal diseases and glaucoma. The well-established 193-nm excimer laser commonly used in refractive surgery is broadly applied because of its exceptional ability to control ablation depth and its minimization of damage to surrounding corneal tissue.[1] The development of a UV laser with similar precision could be of use in the treatment of vitreoretinal diseases and glaucoma because it may reduce the risk for damage to surrounding healthy tissue and complications that may be encountered with the current microsurgical management of these diseases. Complications that arise from unintended damage to surrounding tissue include hemorrhage with vitreoretinal surgery,[2] unpredictable IOP outcomes, and possible hypotony in glaucoma surgery.

Potential applications of various wavelengths, laser parameters, and delivery devices for intraocular surgery have been investigated.[3–6] The delivery of UV laser radiation to intraocular tissue requires the use of a conduit to transport the laser radiation directly to the tissue site. Articulated arms,[7,8] hollow core light guides,[4] and optical fibers[6] have been used in conjunction with various UV wavelengths. In addition to vitreoretinal application,[7] UV lasers have been studied in clinical trials of photoablative filtration for patients with glaucoma and have shown encouraging results.[9–13] A 308-nm XeCl excimer laser used for laser trabecular ablation showed distinct advantages such as reduced levels of collateral damage, avoidance of conjunctival scarring, and modest lowering of intraocular pressure (IOP).[9,11,12] An argon fluoride excimer laser (193 nm) has been used to reduce IOP in patients with open-angle glaucoma through an ab externo approach to photoablative filtration surgery.[10,13] According to the short-term results of the pilot study, this technique seems to have potential applications in clinical ophthalmology. These experimental studies have not found widespread applications, partly because of the complex nature of the required delivery systems. Optimization of laser properties and system design is required if such techniques are to be widely used in clinical ophthalmology. Additionally, the ablation characteristics in a fluid environment are different from those in a gaseous environment.[3,14] Infrared sources such as CO_2, erbium:YAG and holmium:YAG lasers have been studied in clinical trials, through optical fiber delivery, for intraocular surgery.[15–17] Collateral damage to surrounding tissue by thermal and shock-wave effects, however, have limited the application of these lasers in a clinical setting. The femtosecond laser (titanium-sapphire), with its ultrashort pulses, has recently been investigated as a potentially useful tool for laser trabecular ablation that may ablate tissue without significant thermal diffusion, shock propagation, or cavitation.[5] A major advantage of such a laser is that the 800-nm wavelength—a wavelength that transmits well through the cornea and aqueous humor—can be delivered to the trabecular meshwork through a gonioscopic lens. However, this technique requires precise focusing on the target tissue through multiple media and interfaces. High power levels and rapid pulse rates may be required to produce tissue ablation.

Recent advances in the laser-to-optic fiber delivery system, combined with advances in the availability of UV-transmitting optical fiber, provide a significant opportunity to develop systems capable of UV-mediated tissue ablation in the intraocular environment.[18,19] Current challenges include the need to integrate the optic fiber and laser wavelengths to allow sufficient power delivery and to achieve controlled ablation with minimal collateral damage to surrounding tissues. In general,

From the [1]Centre for Ophthalmology and Visual Science, The University of Western Australia, Perth, Australia; and the [2]Australia Link Laboratory, EENT Hospital, Shanghai Medical College, Fudan University, China.

Supported by the National Health and Medical Research Council of Australia and the ARC Centre of Excellence in Vision Science.

Submitted for publication November 4, 2008; revised January 12, March 4 and 18, 2009; accepted June 4, 2009.

Disclosure: **X.-B. Yu**, None; **J. Miller**, None; **P.K. Yu**, None; **S.J. Cringle**, None; **C. Balaratnasingam**, None; **W.H. Morgan**, None; **D.-Y. Yu**, None

The publication costs of this article were defrayed in part by page charge payment. This article must therefore be marked "*advertisement*" in accordance with 18 U.S.C. §1734 solely to indicate this fact.

Corresponding author: Dao-Yi Yu, Centre for Ophthalmology and Visual Science, The University of Western Australia, Nedlands, Perth, Western Australia 6009; dyyu@cyllene.uwa.edu.au.

shorter UV wavelengths have shorter penetration depths but have a greater potential to damage the optic fiber delivery system.[20,21]

We have previously succeeded in delivering 266-nm laser light through optic fibers and have used this wavelength to ablate retinal tissue and vascular sheath tissue at the arteriovenous crossing point.[18,19] The present study extends the work using 266-nm radiation and examines the properties of 213-nm radiation, which can also be generated from a solid state laser and delivered through a flexible fiber-optic probe suitable for intraocular work. We compared the performance of 266-nm and 213-nm wavelengths in ablating porcine retinal tissue. The better performing 213-nm wavelength was then used to assess the ablation properties of human trabecular meshwork with a view to using such technology to ablate channels through to Schlemm's canal in glaucoma surgery. The ability to cut intraocular tissue in a more precise manner would also open up new techniques for a wide range of other intraocular procedures.

METHODS

Tissue Preparation

All experiments were conducted and all laboratory animals were treated in accordance with the ARVO Statement for the Use of Animals in Ophthalmic and Vision Research. All human tissue was handled according to the tenets of the Declaration of Helsinki. The study was approved by the University of Western Australia Animal Ethics and Human Ethics Committees.

Porcine Tissue

Porcine retinal tissue from 20 pig eyes was used to determine the capability of 266-nm or 213-nm laser pulses to ablate ocular tissue. Pig eyes freshly obtained from a local abattoir were placed in oxygenated Ringer's solution and transported to the laboratory on ice. These eyes were carefully dissected, in ice-cold Ringer's solution, into segments with the retina, choroid, and sclera intact. The vitreous was removed, and segments were kept in oxygen-bubbled Ringer's solution at 4°C until use within 3 hours of dissection. During irradiation the segments were pinned to a wax plate immersed in balanced salt irrigation solution (BSS; Alcon Laboratories, Inc., Forth Worth, TX) at room temperature.

Human Tissue

Human trabecular meshwork tissue from four donor eyes was used for testing the ablation capability of the 213-nm laser wavelength. Trabecular meshwork tissue was obtained from human donor eyes provided by the Lions Eye Bank of Western Australia (Lions Eye Institute, Western Australia). Two of the four eyes studied were those of a patient who was a glaucoma suspect 18 years ago and who had increased IOP in both eyes (23 mm Hg in the right eye and 26 mm Hg in the left eye). IOP was maintained at less than 20 mm Hg in both eyes with topical medication, and disc appearance was normal with no subsequent change with follow-up. The visual field had some possible alterations consistent with a left inferior nasal step detected by Humphrey visual field; however, this did not change with follow-up. There was no history of laser or other filtering surgery. The trabecular meshwork had no detectable histopathologic changes at the light microscope level. Eyes had been fixed in 4% paraformaldehyde before use in this study. Anterior chamber angle tissue was first dissected from the eye and then divided into 4-mm-wide pieces. Each piece was immersed in balanced salt irrigation solution at room temperature during laser application.

Laser Parameters

A schematic diagram of the experiment arrangement is shown in Figure 1. Laser and associated optics enabled pulsed ultraviolet laser radiation to be delivered to the tissue surface through an optical fiber; the system is a development of one previously reported.[18] The fourth (266-nm) or fifth (213-nm) harmonic of a pulsed Nd:YAG laser (Surelite II10; Continuum, Santa Clara, CA) was launched into an optical fiber using a custom-made hollow glass taper as a beam concentrator.[19] The 266-nm and 213-nm pulse durations last 4 to 6 nanoseconds, and each harmonic was only used in isolation; the beam not in use was terminated by a beam stop. Beam energy was measured using calibrated laser energy meters (Gentec QE25 and ED100AUX; Gentec Electro-Optics, Quebec, Canada). A low-power 633-nm HeNe laser (Uniphase, Milpitas, CA), colinear with the 266-nm or 213-nm beam, was also launched into the optical fiber as an alignment aid. A key difference between the current and previously reported systems was the smaller diameters of the optical fiber–tapered tips used in this investigation. Although all current and previous fibers were made from the same material and had identical numerical apertures, the smaller tip diameter resulted in a greater rate of fluence reduction with distance from the face of the optical fiber tip and, therefore, affected the depth profile of ablated lesions.

Two types of silica/silica optical fibers were used. One was standard silica/silica (FVP; Polymicro Technologies, Phoenix, AZ) for the delivery of 266 nm radiation, and the other was silica/silica fiber manufactured from a modified preform (FDP; Polymicro Technologies) for the delivery of 213 nm radiation. Fibers lengths were cleaved, waists were formed by propane flame pulling, and neck-down tapers were formed by flame pulling and subsequent cleaving. For the ablation of porcine retina, a range of optical fibers with tapered tips was used. These fibers all had core diameters of 200 μm, lengths between 590 and 1860 mm, and tips tapered where the tip diameter was between 31 and 56 μm. For ablation of the human trabecular meshwork, a range of 600-μm core diameter fibers with tapered tips were used (length, 330–630 mm; tip diameter, 52–71 μm). The shorter lengths and larger core diameters of the later fibers enabled greater fluence to be output from the tapered fiber tip.

Lesions were generated by placing the tissue horizontally on a stereotaxic table (Stellar, Stoelting, IL), lowering the vertical optical fiber tip onto the tissue surface, and irradiating. Retinal lesions were generated using 1, 3, or 10 pulses of 213-nm or 266-nm radiation. Fluence values of 0.1, 0.2, 0.4, 0.6, 0.8, or 1.0 J/cm^2 of 213 nm or 0.2, 0.4, 0.6, 0.8, 1.0, 2.0, 3.0, or 4.0 J/cm^2 of 266 nm were used. Typically, 18 lesions were generated on each tissue segment, with a total of more than 240 lesions generated and sectioned. The horizontal (*xy*) position of the table was controlled to within 0.05 mm, and the vertical (*z* axes) position of the optical fiber tip was controlled to within 0.5 μm with a piezoelectric microdrive (Inchworm; Burleigh Instruments, Fishers, NY).

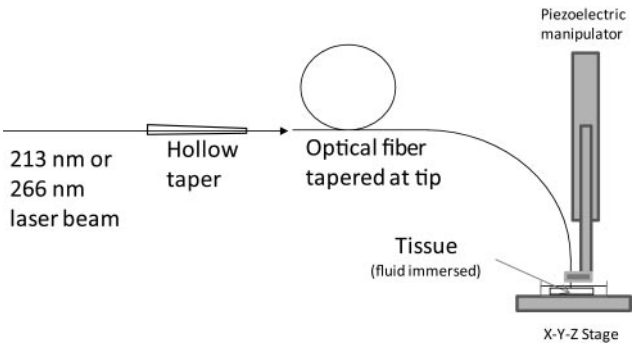

FIGURE 1. The fourth (266-nm) or the fifth (213-nm) harmonic of a pulsed Nd:YAG laser was concentrated through a hollow glass taper before launch into an optical fiber. Unused harmonic was terminated with a beam stop. The optical fiber, with a tapered tip, was orientated and positioned normally to the tissue surface using a piezoelectric manipulator mounted on a stereotaxic device. Target tissue was fluid immersed and placed on an X-Y-Z stage.

Lesions were generated in human trabecular meshwork tissue using 1, 10, or 50 pulses of 213-nm laser radiations with fluence values of 0.05, 0.25, 0.45, 0.65, 1.0, or 1.3 J/cm^2. Typically, 15 lesions were tested in each tissue segment, and four segments were obtained from each eye. As with the porcine retina, the tissue was mounted horizontally on a stereotaxic table. The iris was cut to expose the trabecular meshwork, and the tissue was pinned down during lesion generation. The fiber was positioned to be perpendicular to the trabecular meshwork directly above Schlemm's canal. After irradiation, the tissue segments were further fixed by immersion in 2.5% glutaraldehyde for 24 hours, embedded in epoxy, and transversely sectioned before staining with toluidine blue.[22] Lesion sites were examined and imaged under a microscope (E800; Nikon, Tokyo, Japan) coupled with a high-resolution digital imaging camera (DXM-1200; Nikon). A resolution of 0.09 μm per pixel was obtained when using $\times$40 objectives. The lesions were examined using a software package (Image-Pro Plus, version 5.1; Media Cybernetics, Bethesda, MD). In all cases lesion depth was determined to be the depth from the surface to the deepest point in a direction perpendicular to the fiber output face. For all lesions, a surface line was created by extrapolating the surface from the tissue surface on either surface of the lesion. For retinal lesions, depth was determined using vertical depth to the deepest point. For trabecular meshwork lesions, where the base of the lesion was often irregular, a line across the average base of the lesion was drawn, and a line parallel to the axes of the optical fiber was drawn connecting the surface and base enabling the lesion depth to be determined.

Statistical Analysis

All statistical analysis was performed with commercial software (SigmaStat, version 3.1; SPSS, Chicago, IL). Before analysis, Kolmogorov-Smirnov testing was used to determine whether data were normally distributed. Normally distributed data were analyzed using analysis of variance (ANOVA) with post hoc factor comparison. Nonnormally distributed data were analyzed using ANOVA on ranks with the Tukey test. Mean values are expressed as mean $\pm$ SE.

Porcine retinal ablation and human trabecular meshwork ablation experiments were analyzed separately. For retinal ablation experiments, ANOVA was used to assess the effect of fluence value and number of pulses on parameter *ablation depth*. A separate analysis was performed for each of the 213-nm and 266-nm data. To compare data between the 213-nm and 266-nm groups, ANOVA was used to assess the effect of wavelength (213 or 266 nm), fluence value, and number of pulses on parameter *mean ablation depth*. For trabecular meshwork experiments, ANOVA was used to assess the effect of fluence value and number of pulses on parameter ablation depth.

Results

Retinal Ablation with 266-nm and 213-nm Laser Wavelengths

Side-by-side examples of laser ablation with 266-nm and 213-nm wavelengths in porcine retina are shown in Figure 2. The data shown are for 10 pulses at fluence levels of 0.6, 0.8, and 1.0 J/cm^2. The 213-nm wavelength produces a deeper, cleaner ablation channel than the 266-nm wavelength at the same fluence level.

Examples of ablated lesions produced using pulsed 266-nm laser radiation on porcine retina are shown in Figure 3 for 1, 3, or 10 pulses. Data are shown for fluence levels of 0.6 J/cm^2 and higher, when ablation becomes more clearly visible. In general, ablation depth increased with fluence level. Lesions generated using 10 pulses of the higher fluence showed substantial disruption to the outer retina and distortion of the inner retina,

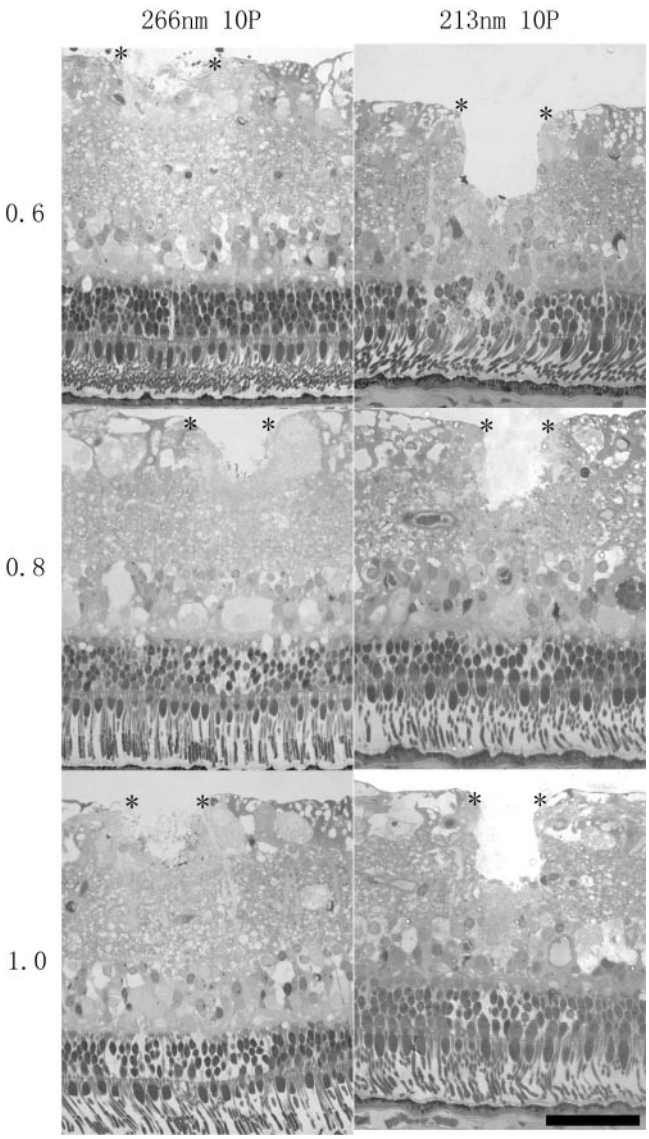

Figure 2. A side-by-side comparison of ablation characteristics of 266-nm and 213-nm laser ablation of porcine retinal tissue after 10 pulses at fluence levels of 0.6, 0.8, and 1.0 J/cm^2. The 213-nm laser creates deeper ablation channels with cleaner demarcation between ablated and remaining tissue and less tissue debris. *Asterisks*: borders of the laser lesions. Scale bar, 50 μm.

rendering measurement of ablation depth unreliable. Data from 10 pulses at fluence levels of 3 J/cm^2 and higher were, therefore, excluded from further analysis.

The mean depth of retinal ablation for six lesions at each fluence level and number of pulses of 266-nm laser radiation is shown in Figure 4. Retinal ablation depth increased significantly with each increment in fluence level ($P < 0.001$) except between fluence levels of 3 J/cm^2 and 4 J/cm^2 ($P = 0.105$). Ablation depth also increased with number of pulses applied, though this effect became insignificant at higher power levels ($P < 0.001$).

Examples of ablated lesions produced using pulsed 213-nm radiation on porcine retina are shown in Figure 5. Fluence levels of 0.2 J/cm^2 and higher caused tissue ablation. The depth of the ablation increased with the fluence level and with the number of pulses applied. Higher magnification sections are shown in Figure 3B; each was generated using 10 pulses with

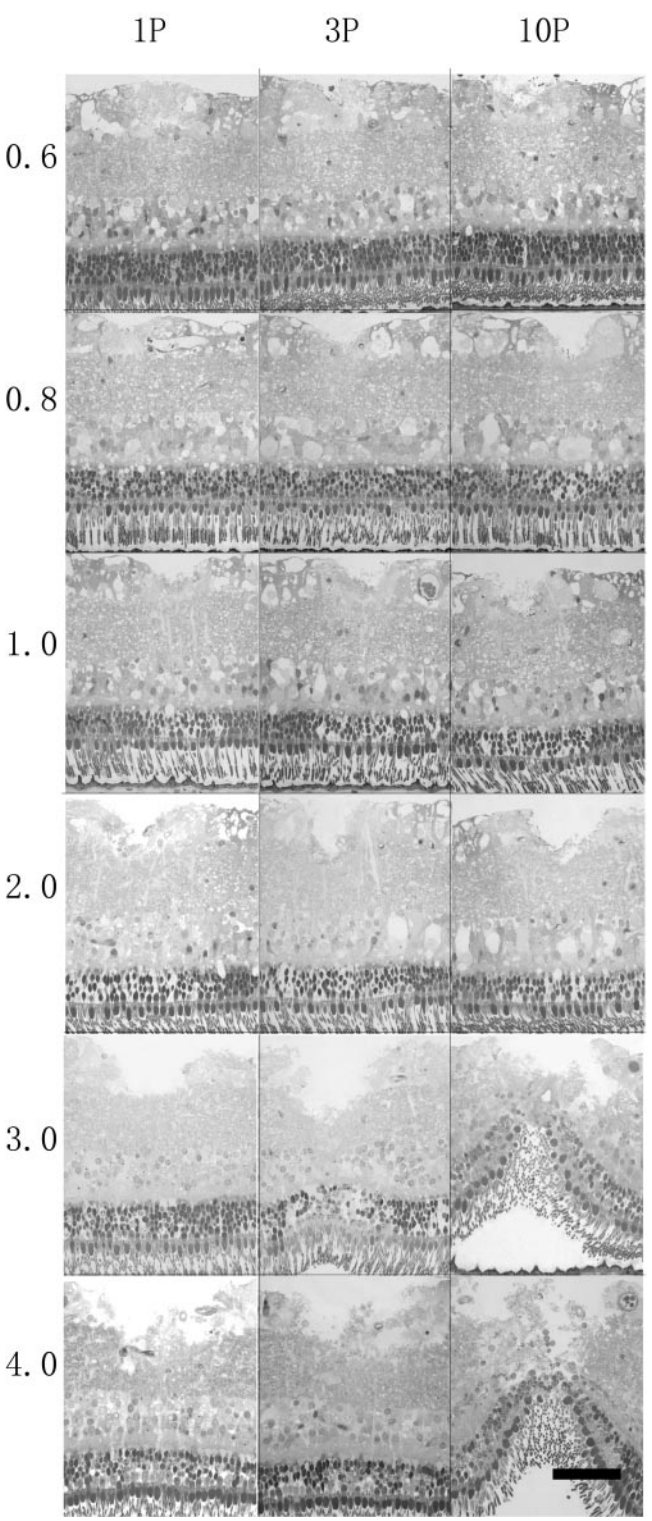

FIGURE 3. Representative sections from porcine retina exposed to a range of fluence levels (0.6–4.0 J/cm^2) and pulse repetitions (1, 3, and 10 pulses) of 266-nm laser radiation delivered through a fiber-optic taper with a tip size of 31 to 56 μm. Ablation depth increases with fluence level, but less so with increasing pulse repetitions. With 10 pulse repetitions (10P) and fluence levels of 3 J/cm^2 and higher, severe damage to the outer retina was evident. Because of the difficulty of determining ablation depth under such circumstances, no attempt was made to quantify ablation depth, and these fluence levels with 10 pulses were excluded from further analysis. Scale bar, 50 μm.

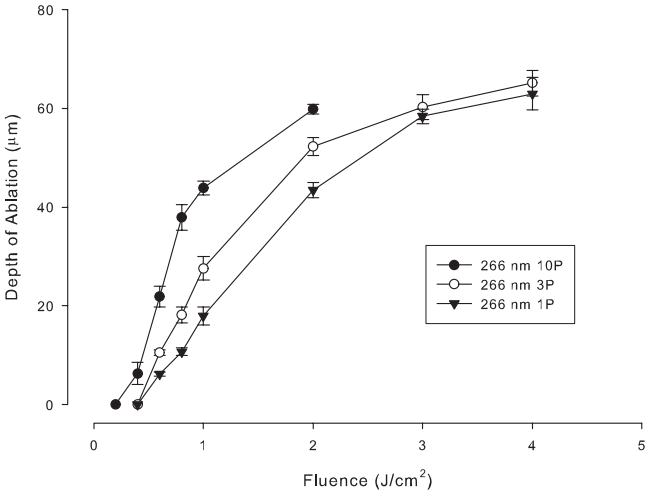

FIGURE 4. Mean retinal ablation depth as a function of fluence level of the 266-nm laser radiation with 1 (1P), 3 (3P), or 10 (10P) pulse repetitions. At lower fluence levels there was a reasonably linear relationship between ablation depth and laser fluence. However, at higher fluence levels the relationship tapered off, and pulse repetition made relatively little difference to resulting ablation depth.

a fluence level of 0.2, 0.6, or 1.0 J/cm^2. The edges of the ablated area were more clearly defined, and had significantly less collateral damage, than those generated using 266-nm laser radiation. Lesions generated using 266-nm laser radiation (Fig. 2) had more tissue debris, a V-shape ablation zone, and more evidence of damage to surrounding tissue than seen in lesions generated using 213-nm laser radiation.

Average data from six to nine lesions generated using 213-nm laser radiation are shown in Figure 6. Mean ablation depth increased with fluence level in an approximately linear fashion. Mean ablation depth also increased with pulse count, but to a lesser extent ($P < 0.05$). Lesions generated using the maximum 213-nm fluence available (1 J/cm^2) had a mean retinal ablation depth for a single 213-nm pulse of 43.8 $\pm$ 1.7 μm, which increased to 54.3 $\pm$ 2.9 μm for lesions generated using 10 pulses. Lesions generated using the same fluence level but with 266-nm laser radiation had a mean ablation depth for a single pulse of 18.0 $\pm$ 1.8 μm, increasing to a mean retinal ablation depth of 43.9 $\pm$ 1.4 μm for lesions generated using 10 pulses. For all fluence levels that produced tissue ablation, a greater mean retinal ablation depth was produced using 213-nm laser radiation ($P < 0.001$).

Trabecular Meshwork Ablation with 213-nm Laser Wavelength

Because the 213-nm laser produced deeper ablation in retinal tissue for a given fluence level and less collateral damage than the 266-nm laser, we used the 213-nm laser for human trabecular meshwork studies. Using the shorter lengths of larger core diameter fibers enabled the maximum fluence output to be increased to 1.3 J/cm^2. Figure 7 shows examples of trabecular meshwork ablation over the fluence range from 0.25 to 1.3 J/cm^2 with 1, 10, or 50 pulses. With high fluence levels and pulse counts, there was considerable ablation of the trabecular meshwork and relatively clean boundaries between the ablated region and the surrounding tissue.

Mean ablation depths of 12 to 14 lesions in human trabecular meshwork at each fluence level and number of pulses of 213-nm laser radiation are shown in Figure 8. The

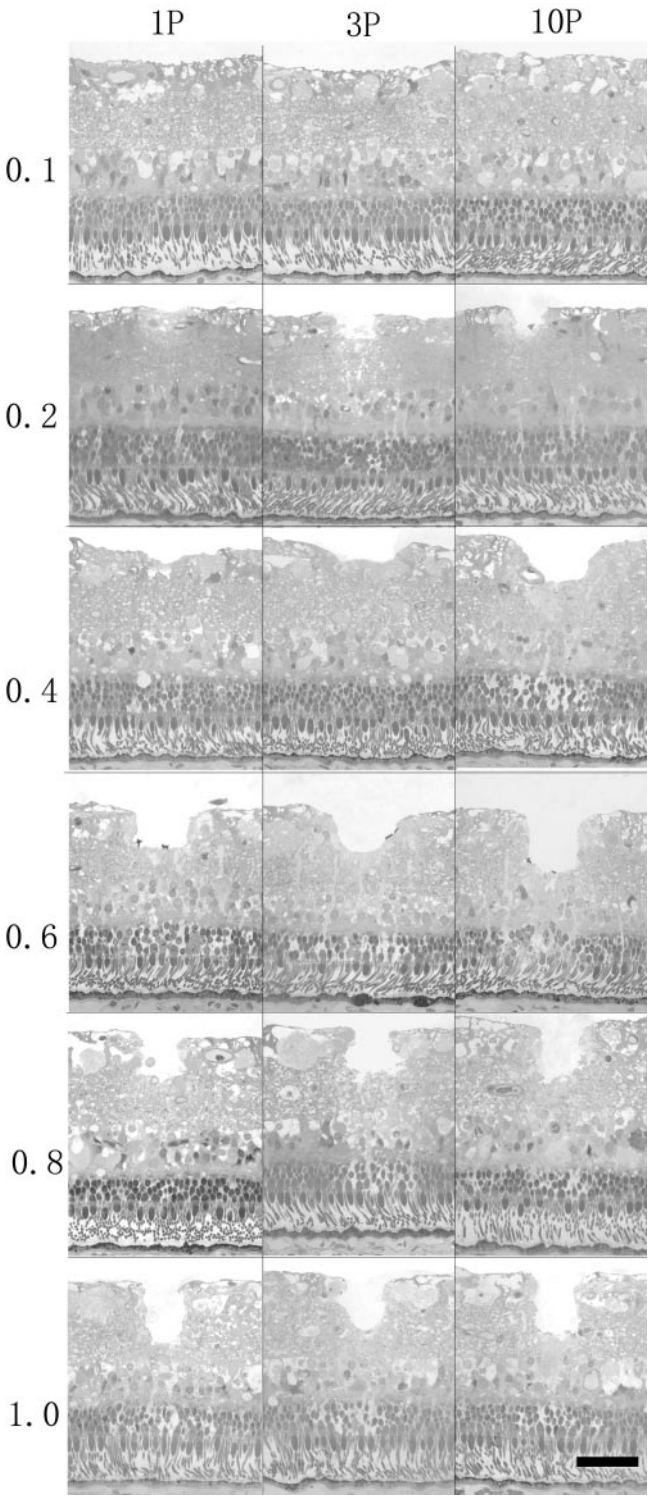

FIGURE 5. Representative sections of porcine retina exposed to a range of fluence levels and pulse repetitions of 213-nm laser radiation. Ablation depth increased with fluence level and number of pulses. The borders of the ablation zone were cleaner than those produced with 266-nm laser radiation, and less debris and less damage to surrounding tissue were evident. Scale bar, 50 μm.

ablation depth of trabecular meshwork was linearly related to fluence level, and ablation depth also increased significantly with the number of pulse repetitions ($P < 0.001$). At the maximum fluence level of 1.3 J/cm^2, the mean ablation depth of trabecular meshwork was 15.7 ± 1.4 μm for a single pulse. This increased to 47.5 ± 3.0 μm with 10 pulses and 101 ± 4.6 μm with 50 pulses. Thus, it was clear that high fluence levels of 213-nm laser energy and multiple pulse applications could ablate considerable depth of human trabecular meshwork tissue.

We then sought to determine directly whether such a technique could be used to cut a channel through the trabecular meshwork to reach Schlemm's canal. Such ability could have applications in glaucoma drainage surgery. Figure 9 shows successful attempts to cut a channel through to Schlemm's canal in human donor eyes. The upper panel (Fig. 9A) shows the trabecular meshwork structure and Schlemm's canal in an unoperated eye. The center panel (Fig. 9B) shows a channel cut through to Schlemm's canal. The edges of the channel are reasonably distinct, and there is no obvious damage to the distal wall of Schlemm's canal. In the example shown in the lower panel (Fig. 9C), the ablation has extended to include some of the distal wall of Schlemm's canal.

DISCUSSION

Lasers are in widespread use in clinical ophthalmology; their thermal or ablation properties are used to modify cellular structure and function or to destroy tissue completely. Tissue ablation effects are confined primarily to shorter wavelength lasers that are most typically used on extraocular tissues such as the cornea.

Penetration depth of UV lasers is poor in the ocular media[23]; hence, special measures must be applied when using UV lasers for intraocular work. In the present study, 266-nm and 213-nm wavelengths were used in a fluid environment by guiding the laser energy through an optical fiber delivery system. Our results from retinal tissue ablation showed that the ablated lesions produced using 213-nm laser radiation were better than those produced using 266-nm laser radiation, as judged by the edges of the ablated area, collateral damage, and the linearity of dose-response

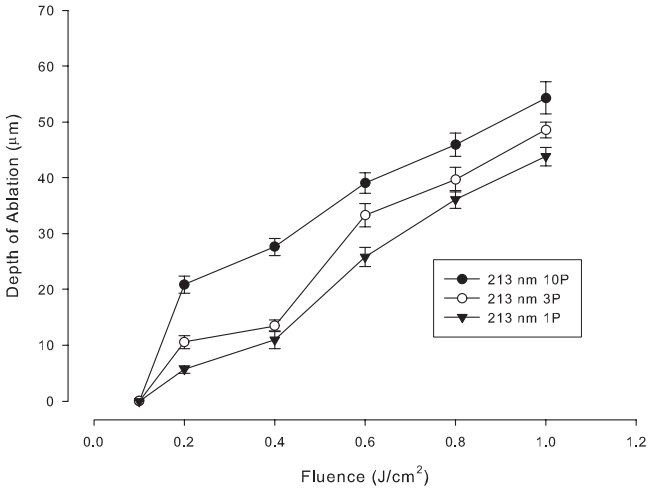

FIGURE 6. Mean retinal ablation depth as a function of the number of pulses and fluence level of the 213-nm laser radiation. Over the range of fluence levels tested, there was a reasonably linear relationship between ablation depth and laser fluence. Ablation depth was greater than that produced with equivalent fluence levels of 266-nm laser radiation.

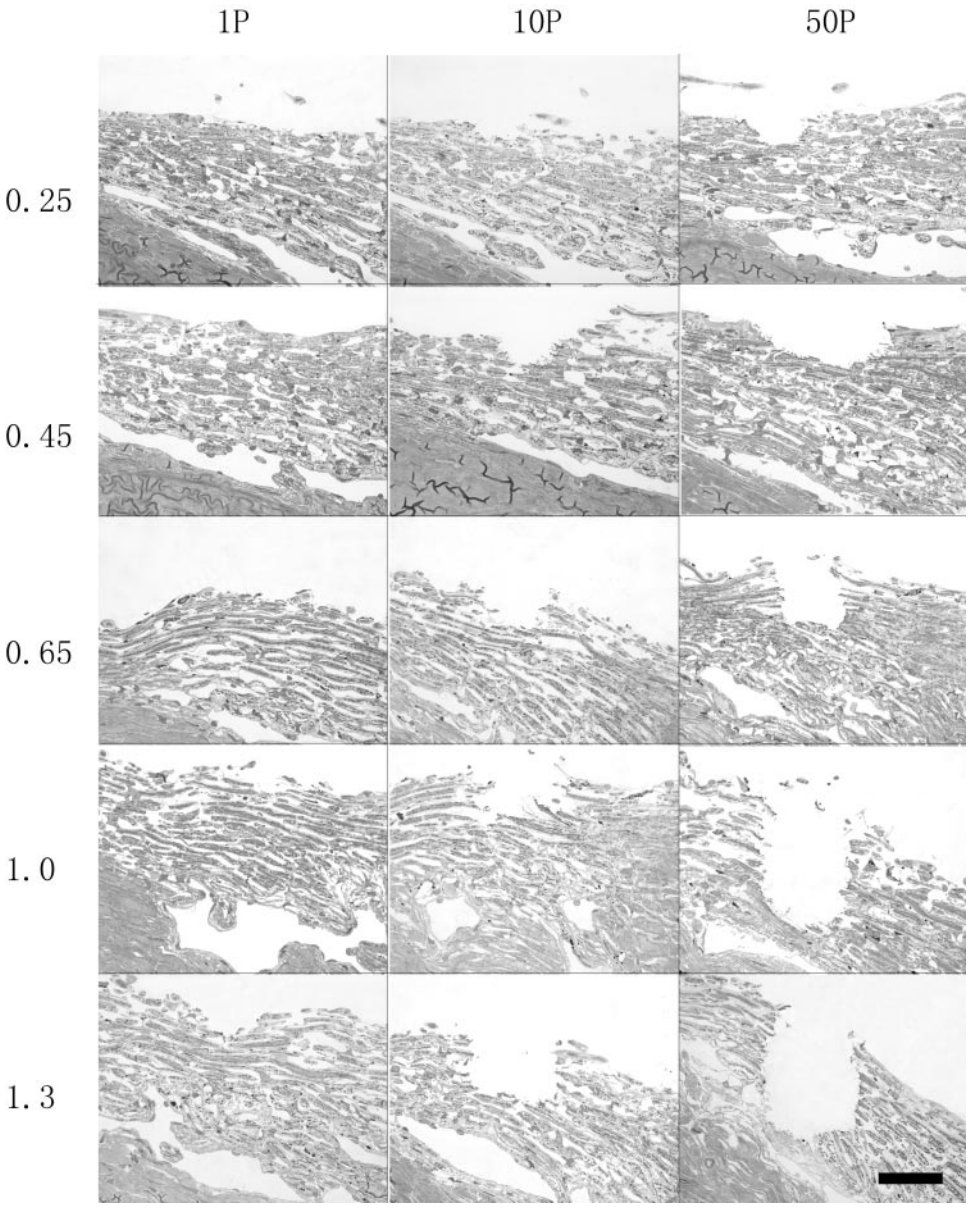

FIGURE 7. Representative sections from human trabecular meshwork exposed to a range of fluence levels and pulse repetitions (1, 10, or 50) of 213-nm laser radiation. Ablation depth generally increased with fluence level and number of pulses. With high fluence levels and 50 pulses, the ablation zone constituted a reasonably clean ablation channel through the trabecular meshwork. Scale bar, 50 μm.

with fluence and number of pulse repetitions. The potential of 213-nm laser radiation to create ablation channels through the human trabecular meshwork was also demonstrated. Work with human trabecular meshwork was restricted to fixed tissue provided by our eye bank from its store of eyes unsuitable for corneal transplantation. We used only those specimens that had morphologically normal trabecular meshworks after dissection. Previous studies of retinal optic coherence tomography in fresh and fixed tissue have suggested that fixation has relatively mild effects on the optical properties of the tissue and that these effects stabilize within 35 minutes of fixation.[24] However, we cannot rule out the possibility that ablation properties of the human trabecular meshwork were affected by fixation. Previous experimental work suggests that the trabecular meshwork and the endothelial cell lining of the inner wall of Schlemm's canal are the primary sites of outflow resistance.[25–27] Bypassing this resistance through laser-created channels in the trabecular meshwork may be a viable procedure for increasing outflow and lowering intraocular pressure. Other potential clinical applications include transection and removal of fibrocellular and fibrovascular membranes and dissection of the vascular sheath at arteriole/venule crossing points in various vitreoretinal diseases. These diseases include retinal detachment with proliferative retinopathy, diabetic traction detachment, penetrating trauma, retinopathy of prematurity, branch retinal vein occlusion, and epimacular membrane.[15]

The present study demonstrated that for the ablation of porcine retinal tissue, 213 nm is a more effective wavelength than 266 nm in terms of lesion definition and efficiency of tissue removal. The 213-nm wavelength also demonstrated the ability to precisely and cleanly remove trabecular meshwork and create a channel to Schlemm's canal.

It is evident that high fluence levels and pulse counts of 266-nm laser can cause significant disruption to the full thickness of the retina (Fig. 3). With 213-nm laser at fluence levels giving a similar rate of tissue ablation, there was no evidence of outer retinal damage (Fig. 5). Use of 213-nm laser wavelengths may, therefore, provide better control of

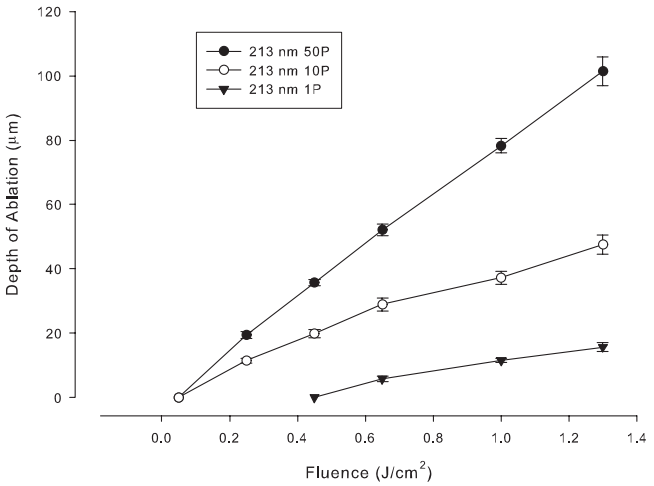

FIGURE 8. Mean trabecular meshwork ablation depth as a function of fluence level of the 213-nm laser with 1 (1P), 10 (10P), or 50 (50P) pulse repetitions. Over the range of fluence levels tested, there was a particularly linear relationship between ablation depth and laser fluence. The depth of trabecular meshwork ablation was also highly dependent on the number of laser pulses delivered.

ablation depth with less collateral damage. We did not have data for matching fluence levels above 1 J/cm^2 for the 213-nm laser; hence, we were unable to determine whether there was a wider window of fluence level without full-thickness damage to the retina with the 213-nm laser. The effect of multiple laser pulses may be influenced by changes in tissue properties created by preceding laser pulses.

It is also evident that over the fluence range and pulse repetitions tested, the 213-nm laser was capable of producing tissue ablation without significant damage to the underlying retina. In contrast, high fluence levels and pulse counts with 266-nm laser exposure was associated with significant full-thickness damage to the retina. Use of 213-nm laser rather than 266-nm laser may provide similar benefits in a clinical setting.

As demonstrated in Figure 9, 50 pulses of 213-nm laser at 1.3 J/cm^2 can ablate through the trabecular meshwork into Schlemm's canal or, in another example, can involve the distal or outer wall of the canal. The inner wall of Schlemm's canal is the target tissue for reducing outflow resistance in the treatment of glaucoma. However, the effect of mild damage to the outer wall of Schlemm's canal is unclear and requires further investigation. It would be important to further study the rate of ablation in a clinical setting to determine the appropriate laser parameters for creating such drainage channels.

Tissue ablation with intraocularly delivered 213-nm laser radiation may have applications in a range of vitreoretinal diseases and in glaucoma filtration surgery.

Acknowledgments

The authors thank Dean Darcey for technical assistance; the staff of the Lions Eye Bank of Western Australia, Lions Eye Institute, for providing human donor eyes; and the staff of DonateWest, the Western Australian agency for organ and tissue donation, for facilitating the recruitment of donors into the study by referral and completion of the consent process.

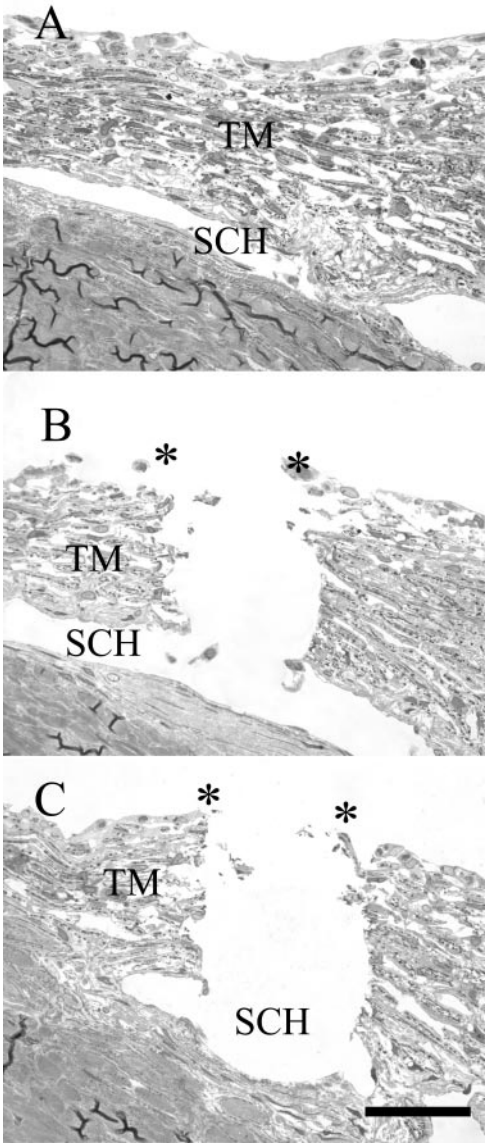

FIGURE 9. Sections of human trabecular meshwork (TM) showing attempts to cut a channel to the Schlemm's canal (SCH). (**A**) Unoperated control. (**B**) Cut through to Schlemm's canal after 50 pulses at a fluence level of 1.3 J/cm^2. (**C**) Slightly deeper cut including some ablation of the distal wall of Schlemm's canal also after 50 pulses at a fluence level of 1.3 J/cm^2. *Asterisks*: borders of the laser lesions. Scale bar, 50 μm.

References

1. Marshall J, Trokel S, Rothery S, Krueger RR. A comparative study of corneal incisions induced by diamond and steel knives and two ultraviolet radiations from an excimer laser. *Br J Ophthalmol.* 1986;70:482–501.
2. Crafoord S, Karlsson N, la Cour M. Sheathotomy in complicated cases of branch retinal vein occlusion. *Acta Ophthalmol.* 2008;86:146–150.
3. Yasukawa T, Yafai Y, Wang Y, et al. Preliminary results of development of a single-mode Q-switched Nd: YAG ring laser at 213 nm and its application for the microsurgical dissection of retinal tissue ex vivo. *Lasers Med Sci.* 2005;19:234–239.
4. Schastak S, Yafai Y, Yasukawa T, Wang YS, Hillrichs G, Wiedemann P. Flexible UV light guiding system for intraocular laser microsurgery. *Lasers Surg Med.* 2007;39:353–357.

5. Toyran S, Liu Y, Singha S, et al. Femtosecond laser photodisruption of human trabecular meshwork: an in vitro study. *Exp Eye Res.* 2005;81:298–305.
6. Herdener S, Pache M. Minimal-invasive glaukomchirurgie:excimer-laser-trabekulotomie. *Ophthalmologe.* 2007;104:730–732.
7. Hemo I, Palanker D, Turovets I, Lewis A, Zauberman H. Vitreoretinal surgery assisted by the 193-nm excimer laser. *Invest Ophthalmol Vis Sci.* 1997;38:1825–1829.
8. Palanker D, Turovets I, Lewis A. Dynamics of ArF excimer laser-induced cavitation bubbles in gel surrounded by a liquid medium. *Lasers Surg Med.* 1997;21:294–300.
9. Wilmsmeyer S, Philippin H, Funk J. Excimer laser trabeculotomy: a new, minimally invasive procedure for patients with glaucoma. *Graefes Arch Clin Exp Ophthalmol.* 2006;244:670–676.
10. Traverso CE, Murialdo U, Di Lorenzo G, et al. Photoablative filtration surgery with the excimer laser for primary open-angle glaucoma: a pilot study. *Int Ophthalmol.* 1992;16:363–365.
11. Vogel M, Lauritzen K, Quentin CD. Targeted ablation of the trabecular meshwork with excimer laser in primary open-angle glaucoma. *Ophthalmologe.* 1996;93:565–568.
12. Vogel M, Lauritzen K. Selective excimer laser ablation of the trabecular meshwork: clinical results. *Ger J Ophthalmol.* 1997;94:665–667.
13. Kumar B, House PH, Morgan WH, Cooper RLC, Allan BDS. The use of 193 nm laser for forming sclerostomies in patients with open angle glaucoma. *Asia-Pacific J Ophthalmol.* 1996;8:2–6.
14. Palanker D, Hemo I, Turovets I, Zauberman H, Fish G, Lewis A. Vitreoretinal ablation with the 193-nm excimer laser in fluid media. *Invest Ophthalmol Vis Sci.* 1994;35:3835–3840.
15. Brazitikos PD, D'amico DJ, Bernal MT, Walsh AW. Erbium:YAG laser surgery of the vitreous and retina. *Ophthalmology.* 1995;102:278–290.
16. Meyers SM, Bonner RF, Rodrigues MM, Ballintine EJ. Phototransection of vitreal membranes with the carbon dioxide laser in rabbits. *Ophthalmology.* 1983;90:563–568.
17. Borirakchanyavat S, Puliafito CA, Kliman GH, Margolis TI, Galler EL. Holmium-YAG laser surgery on experimental vitreous membranes. *Arch Ophthalmol.* 1991;109:1605–1609.
18. Yu PK, Miller J, Cringle SJ, Yu D-Y. Experimental retinal ablation using a fourth-harmonic 266-nm laser coupled with an optical fiber probe. *Invest Ophthalmol Vis Sci.* 2006;47:1587–1593.
19. Miller J, Yu PK, Cringle SJ, Yu D-Y. Laser-fiber system for ablation of intraocular tissue using the fourth harmonic of a pulsed Nd:YAG laser. *Appl Opt.* 2007;46:420.
20. Waynant RW, ed. *Lasers in Medicine*. Boca Raton, FL: CRC Press; 2002.
21. Vogel A, Venugopalan V. Mechanisms of pulsed laser ablation of biological tissues. *Chem Rev.* 2003;103:577–644.
22. Yu D-Y, Su E-N, Cringle SJ, Yu PK. Isolated preparations of ocular vasculature and their applications in ophthalmic research. *Prog Retina Eye Res.* 2003;22:135–169.
23. Boettner EA, Wolter JR. Transmission of the ocular media. *Invest Ophthalmol.* 1962;1:776–783.
24. Chauhan DS, Marshall J. The interpretation of optical coherence tomography images of the retina. *Invest Ophthalmol Vis Sci.* 1999;40:2332–2342.
25. Roberts CJ, Rivera BK, Grzybowski DM, Mahmoud AM, Weber PA. Effect of low fluence diode laser irradiation on the hydraulic conductivity of perfused trabecular meshwork endothelial cell monolayers. *Curr Eye Res.* 2007;32:625–638.
26. Johnson M. What controls aqueous humour outflow resistance? *Exp Eye Res.* 2006;82:545–557.
27. Johnson M, Erickson K. Mechanisms and routes of aqueous humor drainage. In: *Aqueous Humor and the Dynamics of Its Flow.* 2006:2577–2595.